THE ANALYSIS OF THE COMPLIANCE CHANGE PRIOR TO THE ONSET OF CRACK GROWTH

A.Neimitz

Department of Mechatronics and Machines Design, Kielce University of Technology,
Al. 1000 lecia P.P.7, 25-314 Kielce, Poland.

ABSTRACT

Experimental results presented in this paper show that, for certain steels, the compliance of the specimens containing cracks, measured during the partial unloading, decreases during the first stage of loading and reachs the minimum value. After the minimum is reached, the compliance rises along with the growing crack. The theoretical model to find when this situation may happen is presented. Both the experimental analysis and the theoretical model suggest that the minimum is reached for these materials at the onset of the crack growth.

KEYWORDS

Compliance change, stable crack growth, onset of crack growth.

INTRODUCTION

The method of compliance change is considered as one of the most important in the experimental methodology to measure a critical value of the *J*- integral (J_{IC}) or to determine J_R curves. Compliance of the specimen during unloading is a function of the elastic properties of a material as well as the length and the net cross section of the specimen. Growing crack changes the net cross section in front of it thus, the crack extension can be expressed as a function of the compliance change. However, in most cases, the onset of crack growth can not be determined using the compliance change technique. Thus, the value of the J_{IC} determined according to this technique or the potential drop technique is not a value of *J* at the critical moment. It is the value, which is at most, according to certain conventions, close to this point. If one knew the onset of crack growth he would compute the critical value of *J* using the well known, simple Rice's formula [1]. However, according to the author's experimental observations, there are steels, for which the compliance change technique can be used to determine the onset of crack growth. When the pre-cracked specimens made of these materials are repeatedly unloaded from the very beginning of the loading process (displacement control loading process) the reduction of the compliance is first observed until the minimum value is reached.

EXPERIMENTAL OBSERVATIONS

The force, *P*, displacement, *u*, diagrams, *P=P(u),* are always recorded to determine the J_R curves for the specimens containing cracks. The shapes of these diagrams can be classified, according Turner [2], into two groups: *pagoda roof*- type and *round house*-type. As representatives of these groups two steels have been selected: the 40HMNA steel (according to the Polish standards, similar to the ASTM 4340 steel) and the 18G2A steel. The yield stress of the 40HMNA steel varied from 1083 to 1217 MPa, depending on heat

treatment. The ultimate strength varied from 1176 to 1294 MPa, the Ramberg – Osgood exponent, *n*, was equal to 53. The yield stress of the 18G2A steel was 363 MPa, the ultimate strength was 573 MPa and the Ramberg – Osgood exponent was equal to 11. The CCT (central crack tension), DENT (double edge notched tension), SENB (single edge notched bend) specimens were machined and pre-cracked to obtain different in-plane and out-of-plane constraints. For the 40HMNA steel for all heat treatments (quenching and tempering) and for all specimen configurations the shape of the *P=P(u*) diagrams were of the *pagoda roof* type (Fig.1a). For the 18G2A steel the *P=P(u*) diagrams were always of the *round house* shape (Fig.1c).

The analyses of the fractured surfaces of the broken specimens have been performed with the help of the scanning microscope. Characteristic features of these fractographs were always similar. The fractured surfaces of the specimens made of the 40HMNA steel contain both cleavage and ductile domains (Fig.2a). The cleavage domains are distributed either arbitrarily as "islands" surrounded by voided regions or as sequential brittle and ductile regions. The fractographs taken from the specimens made of 18G2A steel indicate a pure ductile mechanism of fracture (Fig.2b) (voids) with shear lips of different size depending on the specimen thickness for the non-side-grooved specimens. Similar fractographs can be presented for side-grooved specimens. The above observations suggest that the shapes of the *P=P(u)* diagrams depend on the mechanism of fracture. From a simple phenomenological model of the specimen containing the growing crack [3] one can conclude that the shapes of the *P=P(u)* diagrams (*pagoda roof* or *round house*) depend on the crack growth equation *a=f(u)* where *a* is an actual crack length. For the very slow crack extension after the onset of crack growth the *round house* shape is observed. For the fast at the beginning and slowing down afterwards crack extension process the *pagoda roof shape* is observed.

The *round house* shape of the *P=P(u)* curves is usually associated with the "plastic" materials for which the large scale yielding is observed in front of the growing crack. The *pagoda roof* shape of the *P=P(u)* curves is usually observed for the small scale yielding in front of the growing crack. The shape of the *P=P(u)* diagrams helps the experimenter to predict the mechanisms of fracture, the general structure of the crack growth equation and, to some extend the microstructure of the material. Moreover, the shape of the *P=P(u)* curves indicates for which materials one can expect the reduction of the compliance of the specimen during unloading before the onset of crack growth. If this reduction is observed, it happens for the materials characterized by the *pagoda roof* shape of the *P=P(u)* diagram. In the Figs 1a and 1b two typical *P=P(u)* curves for the CCT and SENB specimens made of the 40HMNA steel are shown along with the *C=C(u)* diagrams, where *C* is the compliance measured during unloading. In the Fig. 1c the corresponding curve is presented for the 18G2A steel. The minimum of the *C=C(u)* diagrams for the 40HMNA curves can be identified with the onset of the crack growth. It has been confirmed by numerous measurements using the potential drop and multi – specimen techniques. For the *pagoda roof P=P(u)* diagrams the sudden change of the $\Delta\phi=f(u)$ slope (Fig. 3), where $\Delta\phi$ is the potential drop, is observed at the same displacement, *u*. For the *round house P=P(u)* diagrams neither minimum along the *C=C(u)* curves nor the sudden change of the $\Delta\phi=f(u)$ slope can be observed.

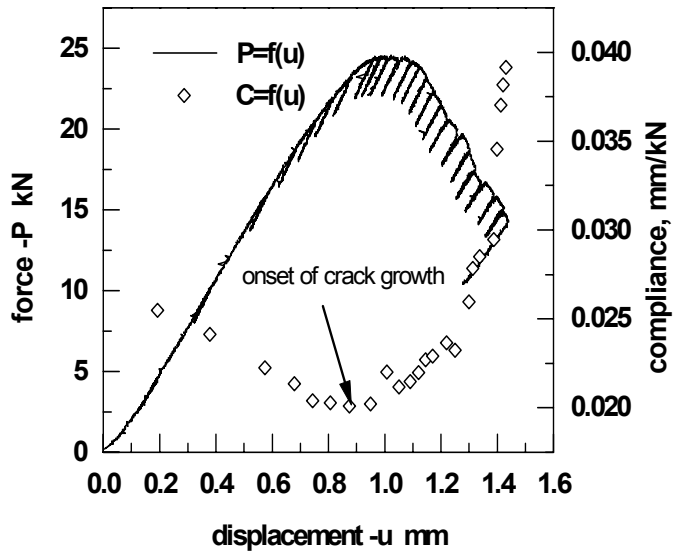

Fig.1a. The *pagoda roof* shape of the *P=P(u)* curve and *C=C(u)* curve. SENT specimen. 40HMNA steel.

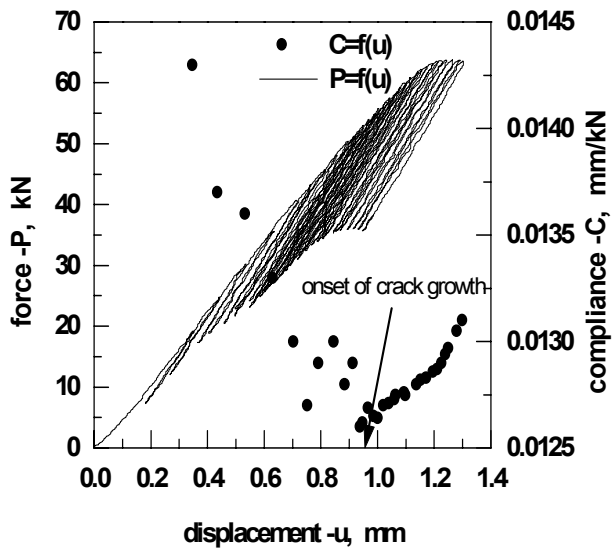

Fig.1b. The *P=P(u)* curve and *C=C(u)* curve. CCT specimen. 40HMNA steel.

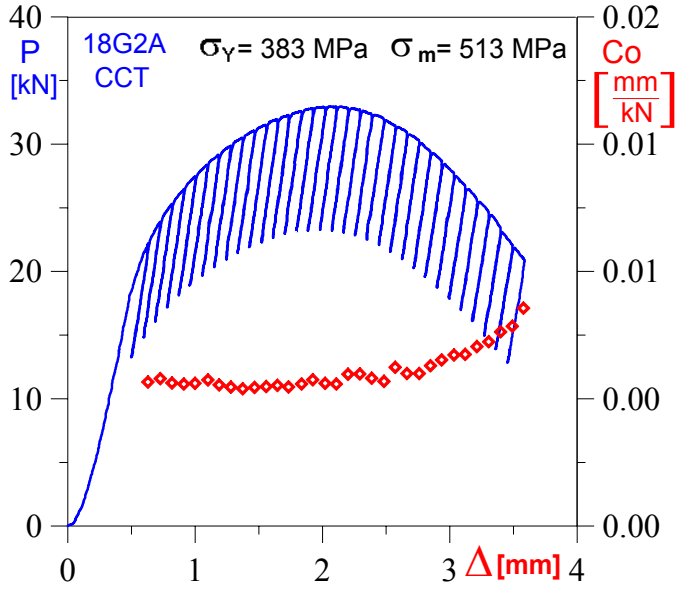

Fig.1c. The *round house* shape of the *P=P(u)* curve and *C=C(u)* curve. CCT specimen, 18G2A steel.

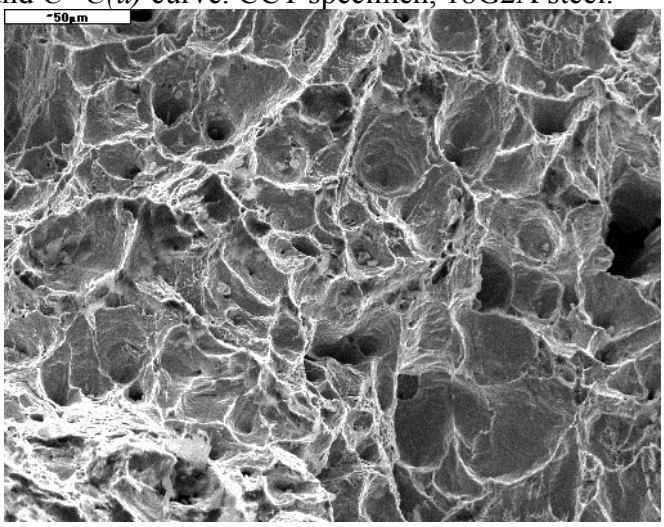

Fig.2a. Fractured surface of the 18G2A steel, SENB specimen.

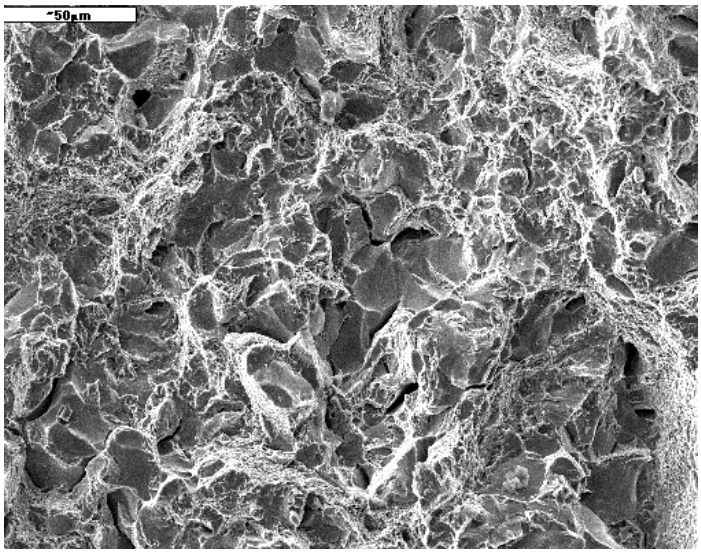

Fig.2a. Fractured surface of the 40HMNA steel, SENB specimen.

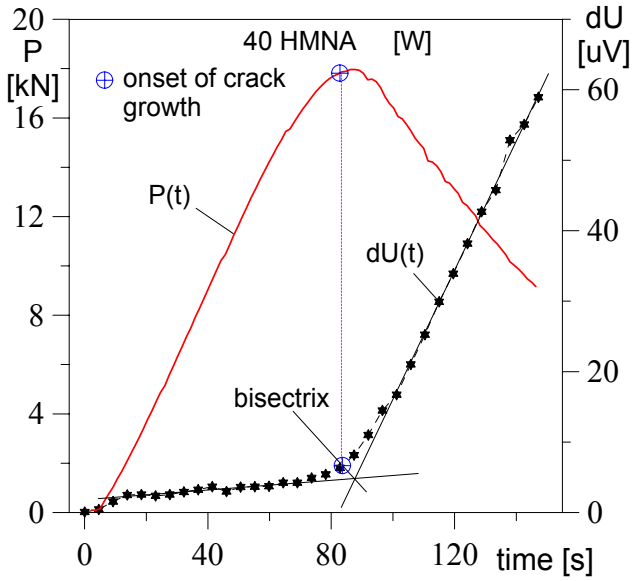

Fig.3. The *pagoda roof house* shape of the *P=P(u)* curve and potential change *Δφ=f(u)* curve

THEORETICAL ANALYSIS

Theoretically obtained *P=P(u)* curves with the help of the phenomenological model [3] are presented in the Figs 4a and 4b. To obtain such curves from the model, the material properties (yield stress, σ_y, the Young's modulus, *E*), geometrical characteristics of the specimen (e.g. for CCT specimens there are: thickness, *B,* width, *2W,* length, *L* and the initial crack length, $2a_0$) and the crack growth equation should be introduced. In the case presented here, the following crack growth equation was used::

$$a(u) = a_0 + \psi u H(u_i - u) + [\psi u_i + \beta(u - u_i)^{\alpha}]H(u - u_i).. \qquad (1)$$

The second term in Eq. (1) represents the blunting process, the third - actual crack growth; α, β, ψ, are some constants (at least in this paper; in general they may be the functions of specimen dimensions and material properties), u_i denotes the load point displacement at the onset of crack growth. *H(-)* is the Heaviside's step function. The power α assumes positive values. In the author's opinion, it may depend on the mechanisms of crack growth.

To obtain the *pagoda roof* shape of the *P=P(u)* diagram, the exponent α should be less than 1 and greater than 1 for the *round house* curves. In the model the point of the crack growth initiation is known thus

it can be precisely pointed out in the *P=P(u)* and *C=C(u)* diagrams. Also the extension of the plastic zone can be traced. From the Fig. 4a one can observe that the minimum along the *C=C(u)* curve coincides with the onset of the crack growth. It is not so for the *round house P=P(u)* diagram (Fig.4b). In this case the very weak minimum along the *C=C(u)* diagram can be observed for the moment of the rapid extension of the plastic zone (in this case the strip yield zone), not at the onset of crack growth. Such a weak minimum can not usually be observed experimentally.

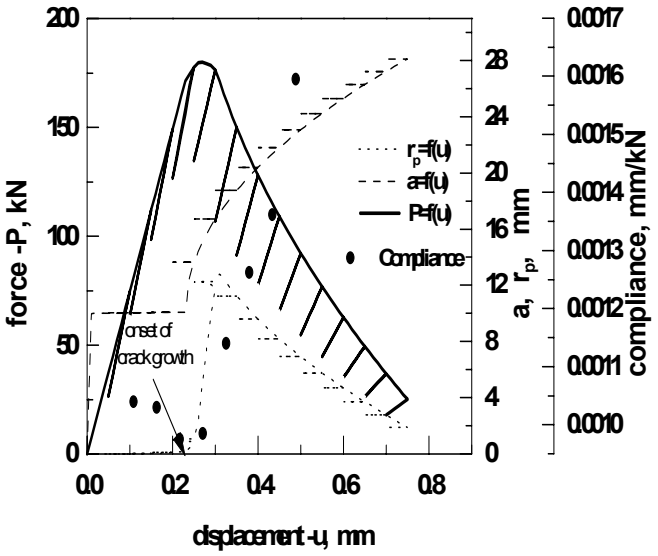

Fig.4a. *Pagoda roof* curve obtained from the phenomenological model. *C=C(u)* points.

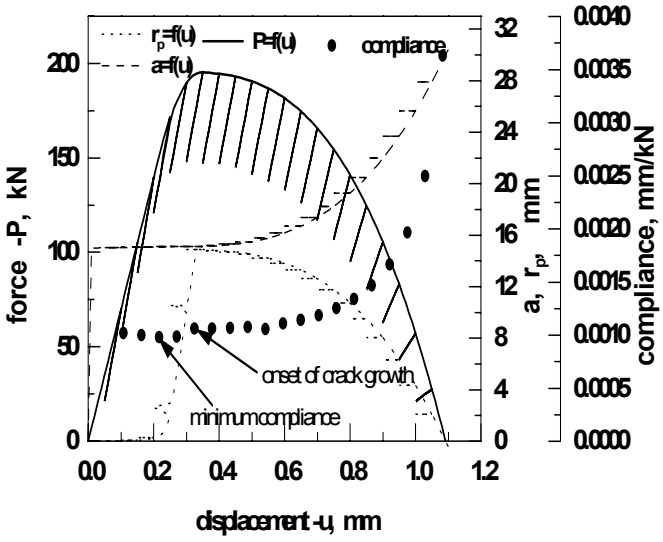

Fig.4b. *Round house* curve obtained from the phenomenological model. *C=C(u)* points.

The theoretical model confirmed the experimental observations. However, there is still the important question open: why it happens? Below, a simple model and computations will be presented. To some extend they answer this question.

When the specimen is loaded the plastic zone evolves in front of the crack. It is assumed first that we observe the small scale yielding situation *SSY*. All computations will be performed for the SENB specimen with the standard proportions for the basic specimen dimensions ($W=2B$, $L=4W$, $0.45<a_0/W<0.65$). The results of the experimental measurements of the compliance for the 40HMNA steel and the SENB specimen are shown in Fig.1a. The SENB has been selected because of very simple basic formulas for the stress intensity factor.

Without the plastic zone in front of the crack the compliance during loading and unloading is constant and can be computed from the formula:

$$C = \frac{u}{P} = \frac{16}{EB}\left(1 + \frac{ah_3 L}{23.28 b_0^2}\right), \tag{2}$$

where $b_0=W-a_0$. To obtain this formula the following procedure and assumptions have been made: It was assumed that the total load point displacement is:

$$u_{Tot} = u_{ncr} + u_{cr}, \tag{3}$$

where: u_{ncr} is deflection of the specimen without a crack, u_{cr} is deflection of the specimen due to the existing crack. To compute u_{ncr} the simplest elementary formula has been used. u_{cr} has been computed from the relation [4]:

$$u_{cr} = \alpha \frac{\sigma_y}{E} a_0 \left(\frac{P}{P_0}\right)^n h_3(n, a/W) \tag{4}$$

Where $n=1$ for an elastic material, P_0 is a limit load which in this case has been computed for the plane strain situation and the Huber-Mises-Hencky yield criterion, h_3 can be found in Kumar et al. [4]. For $0.45<a_0/W<0.65$ this function is equal to a constant: $h_3=4.65$ with the maximum error about 4 per cent.

When the plastic zone is introduced in front of the crack the original crack length can be replaced with the effective crack length.

$$a_{eff} = a_0 + r_p \tag{5}$$

Now, the total deflection of the specimen is:

$$u_{Tot} = \frac{16P}{EB}\left(1 + \frac{(a_0 + r_p)Lh_3}{23.28(b_0 - r_p)^2}\right). \tag{6}$$

We assume the formula for the length of the plastic zone in the form:

$$r_p = \beta\left(\frac{K_I}{\gamma\sigma_y}\right)^2, \tag{7}$$

where $\beta=1/2\pi$ for Irwin's model, $\beta=\pi/8$ for Dugdale's model, γ defines the level of the out-of-plane constraints
. It is equal to unity for plane stress or $\sqrt{3}$ for plane strain situations. More general definition for γ was given by Wang et al. [5]. The formula (6) can also be extended to take into account the effect of strain hardening [6]. Now the "local" compliance during the *loading* process can be written in the form:

$$C_{load} = \frac{du_{Tot}}{dP} = \frac{16}{EB}\left\{\left(1 + \frac{\varepsilon(a_0 + r_p)}{(b_0 - r_p)^2}\right) + 2\beta\varepsilon P\left[\frac{2(a_0 + r_p)}{(b_0 - r_p)^2}\right]\frac{\left(0.995\frac{L}{\sigma_0 B}\right)^2}{(b_0 - r_p)^2(b_0 - 4r_p)}\right\}, \tag{8}$$

where $\varepsilon = \frac{h_3 L}{23.28}$. To compute the compliance during elastic unloading, C_{unl} the following procedure has been assumed: The total energy of the deformation process can be computed from Fig.5 and the formula:

$$E_{Tot} = area(OAC) = Pu_{Tot} - \int_0^P u_{Tot}\,dP. \tag{9}$$

The total elastic energy is equal:

$$E_{elast.} = area(CAB) = \frac{1}{2}C_{unl}P^2. \tag{10}$$

The amount of dissipated energy is equal:

$$E_{dissip.} = area(OAB) = E_{Tot} - E_{elast.} = V_{pl}\xi, \tag{11}$$

where ξ is the average specific energy of the plastic and process zones formation. It is not unreasonable to assume that for the stationary crack and *SSY* this quantity is a constant. The volume of the plastic zone can be approximated by a simple formula:

$$V_{pl} = \psi B r_p^2 . \tag{12}$$

The constant ψ defines how much the shape of the real plastic zone differs from the cylinder. It is also assumed that for the stationary crack and SSY the shape of the plastic zone does not change. Introducing Eqs 9, 10, 12 into Eq.11 one can easily obtain the formula for the compliance during elastic unloading:

$$C_{unl} = \frac{32}{EB}\left[1+\frac{\varepsilon(a_0+r_{pk})}{(b_0-r_{pk})^2}\right] - \frac{32}{P^2}\int_0^P \frac{P}{EB}\left[1+\frac{\varepsilon(a_0+r_{pk})}{(b_0-r_{pk})^2}\right]dP - 2\xi\psi\frac{Br_{pk}^2}{P^2}. \tag{13}$$

The actual length of the plastic zone r_{pk} can be computed by the iterative procedure starting from $r_{p0}=0$. For k=3 the error is less than 3 per cent. Computations has been made for 40HMNA steel with the following data: L=100mm, B=20mm, W=25mm, a_0=12.5mm, E=215000 MPa, σ_y=1100 MPa, ν=0.33. It turns out that the compliance during unloading may increase or decrease depending on the product $\psi\xi$. For the above data this product should be greater than $2\cdot10^4$ MPa in order to observe a decreasing compliance during unloading. The results presented in Fig.6 have been obtained for $\psi\xi=3\cdot10^4$. The above results suggest that the compliance reduction before the onset of the crack growth can be observed if the specific energy of the plastic and process zones formation is sufficiently high.

The computations performed for the same specimen but for the case when the whole ligament is in plastic state (the Kumar et al. [4] formulas were used) do not lead to the compliance change before the onset of the crack growth.

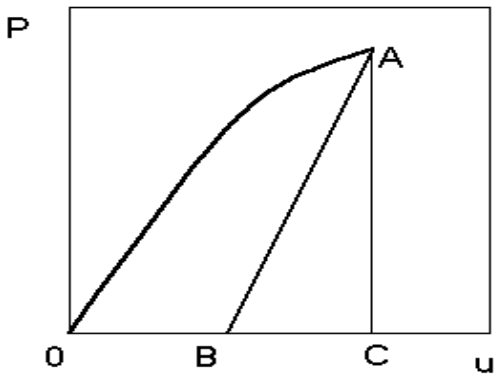

Fig.5. Schematic *P=P(u)* diagram

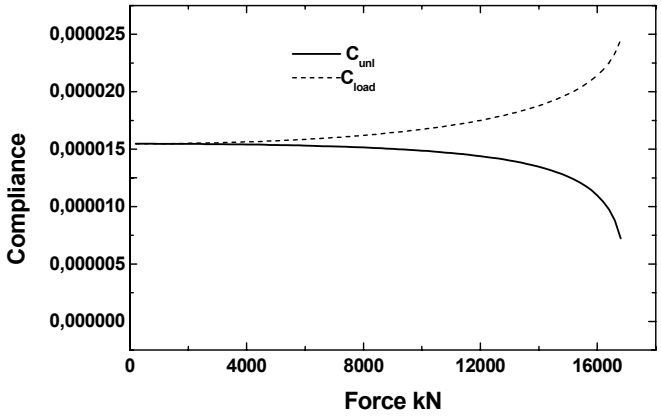

Fig.6. Compliance of the specimen during loading and unloading as a function of the external force

Acknowledgements

Authors gratefully acknowledge support from the Polish National Research Committee, grant No.7 T07C 008 15

REFERENCES

1. Rice, J.R., (1968), *Journal of Applied Mech.*Vol.35, pp.379-386
2. Turner, C.E. (1990) In: Fracture Behaviour and Design of Materials and Structures, 8th European Conference on Fracture (ed. D.Firrao), Vol.II, EMAS, Warley, UK,pp.933-968.
3. Neimitz, A. (2000), In: *Advances in Mechanical Behaviour, Plasticity and Damage,* (Ed. D.Minnay, P.Costa, D.Francois, A.Pineau), Elsevier, Vol.II, pp. 1505-1510
4. Kumar V., German, M.D., Shih C.F. (1981), In: *An Engineering Approach for Elastic Plastic Fracture Analysis,* Electric Power Research Institute, Inc. Palo Alto, Ca, , EPRI Raport NP. – [67]
5. Wang, J., Shen, Y.P., Wanlin, G., (1998), *Engineering Fracture Mechanics*, Vol. 21, pp. 1389-1401,